sciendo

DOI:10.2478/auoc-2019-0011

Ovidius University Annals of Chemistry Volume 30, Number 1, pp. 60 - 64, 2019

The evaluation of kinetic parameters for cadmium doped Co-Zn ferrite using thermogravimetric analysis

Akshay B. KULKARNI,[1] Shridhar N. MATHAD[*],[2] and Raghavendra P. BAKALE[3]

[1]*Department of Physics, Jain College of Engineering, Belagavi, 590014, India*
[2]*K.L.E. Institute of Technology, Hubballi, 580030, India*
[3]*Department of Chemistry, Jain College of Engineering, Belagavi, 590014, India*

Abstract. This work had the objective to analyze the thermodynamic properties of cadmium doped cobalt zinc ferrite ($Co_{0.5}Zn_{0.5}Cd_{0.3}Fe_{1.8}O_4$), obtained by solid state reaction method and characterized by TGA-DTA. The TG analysis show sharp peaks at four points, two for water reduction, one for decomposition of chlorides and last one for formation of end product. The ratio of weight of end product to starting material match with ratio of molecular weight of end product and starting materials; this confirms the formation of ferrite sample. Broido, Coats-Redfern, Chang and Horowitz-Metzger approximations are employed to compute the activation energy (E_a) of formation of ferrite sample. The kinetic parameters like frequency factor (A), entropy change (ΔS), enthalpy change (ΔH) and changes in internal energy (ΔG) of sample are also reported.

Keywords: cadmium doped cobalt zinc ferrites ($Co_{0.5}Zn_{0.5}Cd_{0.3}Fe_{1.8}O_4$), TG-DTA, activation energy, frequency factor.

1. Introduction

Thermogravimetric analysis (TGA) is a thermal analysis technique which assesses the amount and rate of change in the weight of a material as a function of temperature or time in a controlled atmosphere. TGA measurements are used primarily to determine the composition of materials and to predict their thermal stability up to elevated temperatures [1]. Many studies of thermogravimetric data have been used for the determination of kinetic parameters. The thermal degradation of various samples like ferrites/poly (vinylidene fluoride) (PVDF) [2] and $CaCO_3$/PVDF composites [3], zirconia samples [4], carbon nanotubes [5], $Ni_{0.284}Zn_{0.549}Cu_{0.183}Fe_{1.984}O_4$ [6], calcium carbonate [7], and silver nano-particles [8] were reported. The thermal and surface characterization of materials are analyzed using different kinetic models such as Coats–Redfern [9, 10], Horowitz-Metzger [11], Broido [12], Freeman [13], and Chang [14].

The aim of this research is to study the chemical steps of the investigated degradation and the evaluation of the kinetic and thermodynamic parameters by using Coats-Redfern, Horowitz-Metzger and Broido methods. The frequency factor (A), entropy change (ΔS), enthalpy change (ΔH) and changes in internal energy (ΔG) of cadmium doped cobalt zinc ferrite are reported.

2. Experimental

The mixture of chlorides (ferric chloride $FeCl_3{\cdot}6H_2O$, cobalt chloride $CoCl_2{\cdot}6H_2O$, cadmium chloride $CdCl_2{\cdot}H_2O$, and zinc chloride $ZnCl_2$) taken in stoichiometric proportion for the synthesis of cadmium doped cobalt zinc ferrite, $Co_{0.5}Zn_{0.5}Cd_{0.3}Fe_{1.8}O_4$, is finely crushed in agate mortar. The mixture being hygroscopic in nature absorbed atmospheric moisture up to some extent during crushing. Due to presence of moisture content uniformity in mixing is achieved after 30 min. This sample is then used in TGA-DTA. In the reaction process three major end products are expected, out of which two are gas molecules. The synthesis and characterization of studied compound were previously published [15, 16].

3. Results and discussion

3.1. Thermogravimetric and differential thermal analysis

The sample of about 21.467 mg was uniformly spread over the balance pan. The degradation of samples was carried out under oxidizing atmosphere at a flow rate of 20°C/min. From Fig. 1, four major reaction points, at 127, 225, 426, and 715°C, are observed for the given sample. From observations and review of literature we get to the conclusion that the first peak at 127°C is shown for the evaporation of absorbed atmospheric water. The second peak at 225°C is shown for the breaking of coordination bond of water molecule and metal chlorides. From 240-400°C no reactions occurred in the sample and it showed a plateau region. The last peak at 715°C shows the completion of formation process of end product. Above 730°C there is not observed significant change in the sample weight. The active region of formation of ferrite sample is between 426°C (699 K) and 715°C (988 K).

Under air atmosphere, TGA of mixture of ferric chloride $FeCl_3{\cdot}6H_2O$, cobalt chloride $CoCl_2{\cdot}6H_2O$, cadmium chloride $CdCl_2{\cdot}H_2O$, zinc chloride $ZnCl_2$ and absorbed water shows two steps of degradation between 37 to 830°C. The first zone from 37-225°C corresponds to removal of moisture and coordinated water molecules

[*] Corresponding author. *E-mail address:* physicssiddu@gmail.com (Shridhar N. Mathad)

with a total loss of about 56.18%. This initial zone is followed by the plateau region between 250 to 400°C showing the formation of intermediate stable compound with total degradation of 0.40%. The plateau region subsequently followed by the decomposition of chlorides and oxidation zone, from 432 to 740°C with total drop-off of weight by 21.96%. Another plateau region observed beyond 740°C and the residue left is the ferrite end product constitutes a weight of 16.45%.

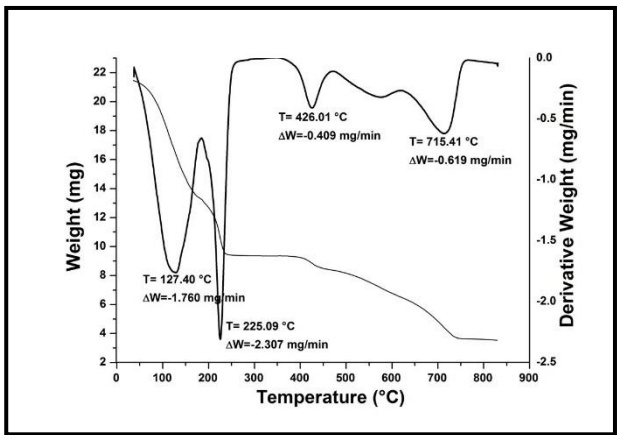

Figure 1. Thermogram of $Co_{0.5}Zn_{0.5}Cd_{0.3}Fe_{1.8}O_4$.

The mixture absorbed atmospheric water molecules due to hygroscopic nature of chemicals used constitutes a large quantity of sample; mixture loses water molecules in two steps and a continuous weight change observed between at 50 to 250°C. The two endothermic peaks are observed, one at 124°C showing evaporation of large quantity of water and another at 228°C showing the breaking of coordinated water molecules. DTG curve shows maximum weight loss at 127 and 225°C. The sample left at 400°C is mixture of metal chlorides, which shows the breaking of chloride molecules at 426°C and shows a continuous decrease in weight till 740°C. The DTG curve indicates maximum change of weight at 426 and 715°C respectively and shows two endothermic peaks at 432 and 740°C showing the beginning of decomposition of chlorides and completion of formation of the end product. Following chloride decomposition and oxidation, another plateau region is observed beyond 740 till 830°C with a loss of 0.95%, and the residue left is the ferrite end product ($Co_{0.5}Zn_{0.5}Cd_{0.3}Fe_{1.8}O_4$) constituting a weight of 16.45%.

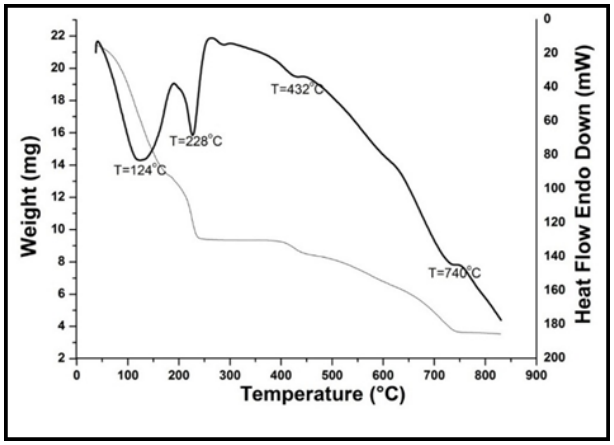

Figure 2. Graph of weight *vs.* temperature and heat flow *vs.* temperature for $Co_{0.5}Zn_{0.5}Cd_{0.3}Fe_{1.8}O_4$.

All four major reactions points at 124, 228, 432, and 740°C show downward peaks in endo-down graph in Fig. 2, indicating reactions require energy, and are endothermic in nature. The increase in heat from 432 to 740°C shows the increase in entropy of system. The increase in entropy observed due to increase in surface area (production of small particles).

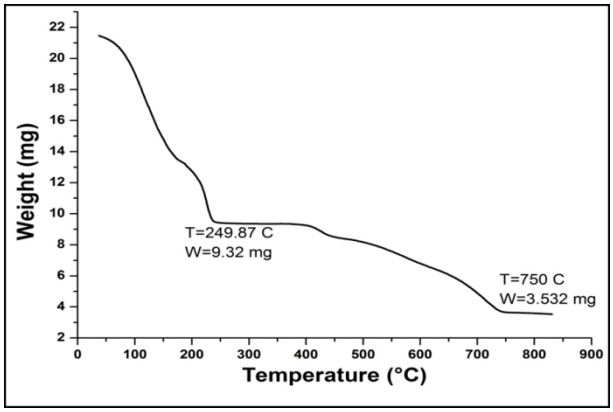

Figure 3. Graph of weight *vs.* temperature for $Co_{0.5}Zn_{0.5}Cd_{0.3}Fe_{1.8}O_4$.

The residue weight versus temperature is plotted as shown in Fig. 3, two plateau regions are observed; one after complete evaporation of all water molecules (atmospheric and coordinated water) and another after formation of end product after completion of reaction. The ratio of molecular weight of starting mixture with dehydrated chlorides and molecular weight of end product is 38.62%, which is matching with ratio of weight of sample at two plateau regions, i.e. 37.89%. This confirms the formation of the end product and accuracy of stoichiometric proportion.

3.2. Coats and Redfern method

From the Coats and Redfern explanation, the mathematical relation for reaction is [9,17-19]:

- for order of reaction $n = 1$

$$\log\left[\frac{-\log(1-\alpha)}{T^2}\right] = \log\frac{AR}{\beta E_a}\left[1-\frac{2RT}{E_a}\right] - \frac{E_a}{2.303RT} \qquad (1)$$

Where: α =fraction of sample decomposed given by the equation

$$\alpha = \frac{W_0 - W_t}{W_0 - W_f} \qquad (2)$$

W_t = weight of sample at any given temperature T (mg); W_o = initial weight of the sample, before the start of decomposition reaction (mg); W_f = final weight of the sample after completion of reaction (mg); $W = W_t - W_f$ (mg); β = rate of heating (20°C/min); T = absolute temperature (K);

-for order of reaction $n \neq 1$

$$\log\left[\frac{1-(1-\alpha)^{1-n}}{T^2(1-n)}\right] = \log\frac{AR}{\beta E_a}\left[1-\frac{2RT}{E_a}\right] - \frac{E_a}{2.303RT} \quad (3)$$

Assuming $n = 1$, a graph of $\log\left[\frac{-\log(1-\alpha)}{T^2}\right]$ vs. 1000/T is plotted as shown in Fig. 4 considering $\log\frac{AR}{\beta E_a}\left[1-\frac{2RT}{E_a}\right]$ remain significantly constant for most

values of E_a and for the temperature range over which reactions generally occur. The slope of straight line gives $-Ea/2.303R$ and intercept can be used for the calculation of frequency factor *A*.

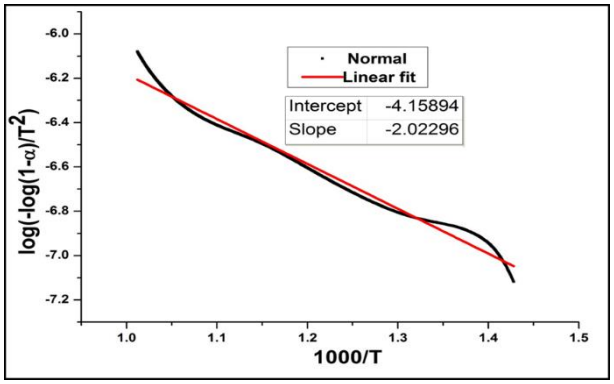

Figure 4. Coats and Redfern plot for $Co_{0.5}Zn_{0.5}Cd_{0.3}Fe_{1.8}O_4$.

The deviation of graph from straight line is observed in the following cases as per literature available: (i) where *n* is slightly different from 1; (ii) when there is slight difference observed at initial weight W_o due to equipment measurement error or moisture content; and (iii) at the starting point and end point of reaction, an observation is seen of deviation from straight line due to errors in α.

By taking R = 8.314 J·mol^{-1}·K^{-1}, β = 20°C·min^{-1}, E_a and A are determined [19].

$$\Delta S = R\ln\left(\frac{Ah}{k_B T}\right) \quad (4)$$

$$\Delta H = E_a - RT \quad (5)$$

$$\Delta G = \Delta H - T\Delta S \quad (6)$$

Where: A = frequency factor, Arrhenius constant, pre-exponential factor (min^{-1}); ΔS = entropy change (J/mol·K); ΔH = enthalpy change (kJ/mol); ΔG = change in internal energy (kJ/mol); k_B = Boltzmann constant (1.38x10^{-23} J/K); E_a = activation energy (kJ/mol); h = Planks constant (J·s); R = universal gas constant (J·K^{-1}·mol^{-1}) and n = order of reaction.

Table 1. Thermodynamic properties from Coats-Redfern and Horowitz-Metzger methods.

Method	Activation energy (kJ/mol)	Frequency factor (min^{-1})	Entropy change (J/mol·K)	Enthalpy change (kJ/mol)	Change in internal energy (kJ/mol)
Coats and Redfern	38.734	6.462	-239.398	30.156	267.041
Horowitz and Metzger	67.347	9.688x10^2	-197.739	59.132	254.499

Entropy change, enthalpy change and change in internal energy are calculated at peak temperature of the reaction T = 988 K for formation of ferrite, and are reported in Table 1.

3.3. Broido method

In the Broido method, Broido used the different approximations and end up with three equivalent following equations [12, 20, 21]:

$$\ln\ln(1/y) = \left(\frac{E_a}{RT_M} + 1\right)\ln T + Constant \quad (7)$$

$$\ln\ln(1/y) = \left(\frac{E_a}{RT_M^2}\right)T + Constant \quad (8)$$

$$\ln\ln(1/y) = -\left(\frac{E_a}{R}\right)\frac{1}{T} + Constant \quad (9)$$

Where: T_M = temperature at which the rate of sample decomposition is maximum (K).

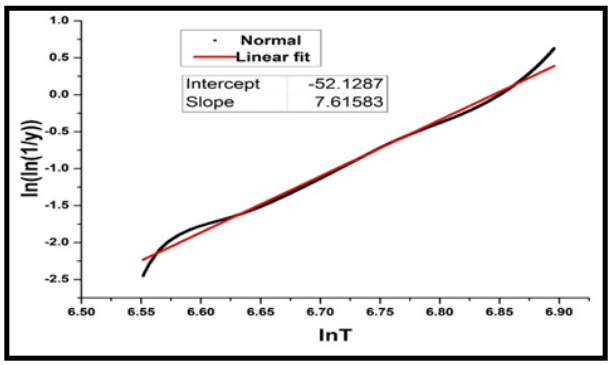

Figure 5. Graph of $\ln\ln(1/y)$ *vs.* lnT plotted using Broido formula for formation of $Co_{0.5}Zn_{0.5}Cd_{0.3}Fe_{1.8}O_4$.

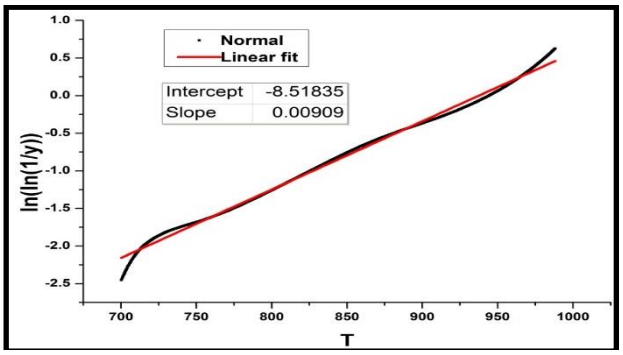

Figure 6. Graph of $\ln\ln(1/y)$ *vs.* T plotted using Broido formula for formation of $Co_{0.5}Zn_{0.5}Cd_{0.3}Fe_{1.8}O_4$.

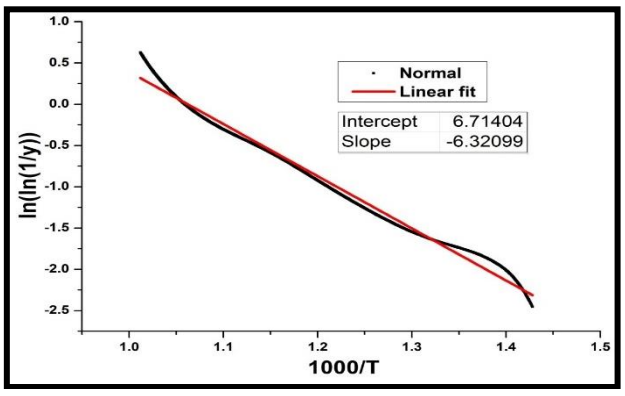

Figure 7. Graph of $\ln\ln(1/y)$ *vs.* 1000/T plotted using Broido formula for formation of $Co_{0.5}Zn_{0.5}Cd_{0.3}Fe_{1.8}O_4$.

All three equations give a linear graph as shown in Figs. 5, 6, 7, but according to Broido approximations the last one, i.e. Fig. 7, is said to be the most accurate. The final equation for determination of activation energy after introduction of correction factor $S(z)$ for Fig. 7 is:

$$E_a = -S(z)R\frac{\Delta[\ln\ln(1/y)]}{\Delta 1/T} \quad (10)$$

Where: y = 1-α given by:

$$y = \frac{W_t - W_f}{W_0 - W_f} \qquad (11)$$

Over the entire range of temperature, $S(z)$ value is assumed to be 0.96. The error introduced by the assumption of constant slope over usual heating range is comfortably less than 10%. The calculation is done by taking the T_M value as 988 K over a range of temperature of 700 to 988 K for ferrite and is tabulated in Table 2.

Table 2. Activation energy values from Coats-Redfern, Broido, Horowitz-Metzger and Chang method.

	Coats and Redfern	**Broido lnln(1/y) vs lnT**	**Broido lnln(1/y) vs T**	**Broido lnln(1/y) vs 1000/T**	**Horowitz and Metzger**	**Chang**
Activation energy (kJ/mol) ($Co_{0.5}Zn_{0.5}Cd_{0.3}Fe_{1.8}O_4$)	38.734	54.344	73.771	51.922	67.347	59.749
R^2 (for graphs plotted)	0.981	0.993	0.995	0.988	0.995	0.957
Std error of estimate	0.0338	0.0628	0.0539	0.0844	0.0539	0.0792
Intercept	-4.159	-52.129	-8.818	6.714	0.059	5.427
Slope	-2.023	7.616	0.009	-6.321	0.009	-7.187
ANOVA Significance	.000	.000	.000	.000	.000	.000

3.3. Horowitz-Metzger method

In Horowitz and Metzger method, Horowitz and Metzger derived equation assuming $\theta/T_s << 1$ where θ is chosen such that $\theta = T - T_s$ [11, 22]:

$$-1 = -\frac{A}{\beta}\frac{RT_S^2}{E_a} e^{-\frac{E_a}{RT_S}} \qquad (12)$$

$$\ln\ln(1/y) = \frac{E_a \theta}{RT_S^2} \qquad (13)$$

$$\theta = T - T_s \text{ (K)} \qquad (14)$$

where: T_s =temperature defined such that at T_s, W/Wo = l/e. When $T = T_s$, $\theta = 0$ and $\ln W/W_0 = -1$.

A graph of equation (14) is plotted as shown in Fig. 8 and activation energy is calculated by taking β as 20°C/min and Ts taken at 944 K for formation of $Co_{0.5}Zn_{0.5}Cd_{0.3}Fe_{1.8}O_4$.

The equations (4)–(6) are used to calculate entropy change, enthalpy change and change in internal energy, and the values are tabulated in Table 1.

3.4. Chang method

From the Arrhenius plot of (ln k/w) versus 1/T using equation (15) as shown in Fig. 9, the slope is equal to $-E_a/R$, where k = rate of weight loss at temperature T, w = corresponding weight of the remaining sample. From the slope ($-E_a/R$) of this plot, activation energy is calculated [14, 23] and the results are tabulated in Table 2.

$$\ln(k/w) = -\frac{E_a}{RT} + cons\tan t \qquad (15)$$

3.5. Standard deviation (σ) and regression (R^2)

The standard deviation can be used to determine the spread out of numbers of activation energy. The standard deviation can be calculated using the following formula:

$$\sigma = \sqrt{\frac{1}{N}\sum_{1}^{N}(E_a - \overline{E_a})^2} \qquad (16)$$

The average activation energy for formation of $Co_{0.5}Zn_{0.5}Cd_{0.3}Fe_{1.8}O_4$ is 57.668 kJ/mol and is tabulated in Table 3. The standard deviation for activation energy calculation is 11.230.

Table 3. Standard deviation for activation energy of $Co_{0.5}Zn_{0.5}Cd_{0.3}Fe_{1.8}O_4$.

	$Co_{0.5}Zn_{0.5}Cd_{0.3}Fe_{1.8}O_4$		
	E_a	$E_a - \overline{E_a}$	$(E_a - \overline{E_a})^2$
	38.734	-18.934	358.490
	67.347	9.679	93.686
	54.544	-3.124	9.758
	73.711	16.043	257.383
	51.922	-5.746	33.015
	59.749	2.081	4.331
		Variance	126.111
$\overline{E_a}$	57.668	Standard deviation	11.230

The regression values of all different graphs are noted in Table 3. The regression values are considerably good. The value of significance for the graphs is .000. They fall in 1% of level of significance. All methods are approximations and have their own limitations of calculation. The variations in results are due to calculation of single TG-DTA data with single heating rate.

4. Conclusions

In the present work, activation energy is determined using four different methods for the first time for cadmium doped cobalt zinc ferrite. The range of variation of activation energy is witnessed to be between 38-74 kJ/mol. The enthalpy change is observed to be positive in the range of 30-60 kJ/mol, indicating the requirement of energy for occurrence of reaction (endothermic); the endothermic nature of reaction is in agreement with the heat flow graph. The entropy change is observed to be large of the order of -200 J/mol·K due to increase in randomness of the system with increase in temperature; this is due to increase in surface area (i.e. formation of small particles). The internal energy is found to be positive and large in the range of 260 kJ/mol, showing that the end product is highly stable compared to the reactant molecules. The change is internal energy for

water till mid plateau region for the sample is also positive showing that intermediate compound in middle plateau region is also stable compared to mixture of starting chemicals.

Conflict of interest

No conflict of interest declared.

References

[1] C. Vovelle, H. Mellottee, J.L. Delfau, Preprints of Papers - American Chemical Society Division of Fuel Chemistry 28 (1983) 291-300.
[2] P. Martins, C. M. Costa, M. Benelmekki, G. Botelho, S. Lanceros-Mendez, Journal of Materials Science 48 (2013) 2681–2689.
[3] J. S. C. Campos, A. A. Ribeiro, C. X. Cardoso, Materials Science and Engineering B 136 (2007) 123-128.
[4] K. Pal, D. J. Kang, Z. X. Zhang, J. K. Kim, Langmuir 26 (2009) 3609-3614.
[5] S. Yu, W. Zheng, W. Yu, Y. Zhang, Q. Jiang, Z. Zhao, Macromolecules 42 (2009) 8870-8874.
[6] R. Balusamy, P. Kumaravel, N. Kanagathara, R. G. S. Rao, N.G. Renganathan, Acta Physica Polonica A 130 (2016) 751-757.
[7] X. G. Li, Y. Lv, B. G. Ma, W. Q. Wang, S. W. Jian, Arabian Journal of Chemistry 10 (2017) S2534–S2538.
[8] T. Greco, F. Wang, M. Wegener, Ferroelectrics 405 (2010) 85-91.
[9] A. W. Coats, J. P. Redfern, Nature 201 (1964) 68-69.
[10] A. W. Coats, J. P. Redfern, Analyst 88 (1963) 906–924.
[11] H. H. Horowitz, G. Metzger, Analytical Chemistry 35 (1963) 1464-1468.
[12] A. Broido, Journal of Polymer Science 7 (1969) 1761-1773.
[13] E.S. Freeman, B. Carroll, The Journal of Physical Chemistry 62 (1958) 394-397.
[14] W.L. Chang, Journal of Applied Polymer Science 53 (1994) 1759–1769.
[15] A. B. Kulkarni, S. N. Mathad, International Journal of Self-Propagating High-Temperature Synthesis 27 (2018) 37–43.
[16] A. B. Kulkarni, S. N. Mathad, Materials Science for Energy Technologies 2 (2019) 455–462.
[17] P. V. Dalal, K. B. Saraf, N. G. Shimpi, N. R. Shah, Journal of Crystallization Process and Technology 2 (2012) 156-160.
[18] P. Šimon, Journal of Thermal Analysis and Calorimetry 76 (2004) 123–132.
[19] C. Li, K. Suzuki, Journal of Thermal Analysis and Calorimetry 98 (2009) 261–266.
[20] M. E. Brown, Introduction to Thermal Analysis Technique and Applications, Chapman & Hall, New York, 1988.
[21] S. Gopalakrishnan, R. Sujatha, Der Chemica Sinica 2 (2011) 103-117.
[22] G. G. Cameron, J. D. Fortune, European Polymer Journal 4 (1968) 333-342.
[23] S. Gul, A. A. Shah, S. Bilal, Journal of Scientific and Innovative Research 2 (2013) 673-684.

Received: 17.01.2019
Received in revised form: 11.05.2019
Accepted: 15.05.2019